Jossinger, S., Yablonski, M., Amir, O, & Ben-Shachar, M. (2023). The role of the cerebellum in language comprehension and production. Neurobiology of Language, Advance publication. https://doi.org/10.1162/nol_a_00098.

The contributions of the cerebellar peduncles and the frontal aslant tract in mediating speech fluency

Jossinger S.[1*], Yablonski M.[1§], Amir O.[2], Ben-Shachar M. [1,3*]

[1] The Gonda Multidisciplinary Brain Research Center, Bar-Ilan University, Ramat-Gan, Israel

[2] Department of Communication Disorders, Sackler Faculty of Medicine, Tel-Aviv University, Tel-Aviv, Israel

[3] Department of English Literature and Linguistics, Bar-Ilan University, Ramat-Gan, Israel

[*] Corresponding author at The Gonda Multidisciplinary Brain Research Center, Bar Ilan University, Ramat Gan 5290002, Israel. E-mail addresses: jossins@biu.ac.il ; michalb@mail.biu.ac.il

[§] Current address at Stanford University School of Medicine and Graduate School of Education, Stanford, CA, USA.

Abbreviated title: Cerebellar contributions to speech fluency

Acknowledgments: This study was conducted as part of Sivan Jossinger's doctoral dissertation, carried out under the supervision of Prof. Michal Ben-Shachar at the Gonda Multidisciplinary Brain Research Center, Bar-Ilan University. The analysis of speech rate data was carried out by Gaya Noam and Michal Braun, under the supervision of Prof. Ofer Amir. We thank Yaniv Assaf, Daniel Barazany and the team at the Strauss Center for Computational Neuroimaging for their assistance in protocol setup and MRI setting.

Conflict of interest: Authors report no conflict of interest

Funding sources: This study is supported by the Israel Science Foundation (ISF Grant #1083/17).

The contributions of the cerebellar peduncles and the frontal aslant tract in mediating speech fluency

ABSTRACT

Fluent speech production is a complex task that spans multiple processes, from conceptual framing and lexical access, through phonological encoding, to articulatory control. For the most part, imaging studies portraying the neural correlates of speech fluency tend to examine clinical populations sustaining speech impairments, and focus on either lexical access or articulatory control, but not both. Here, we evaluated the contribution of the cerebellar peduncles to speech fluency by measuring the different components of the process, in a sample of forty-five neurotypical adults. Participants underwent an unstructured interview to assess their natural speaking rate and articulation rate, and completed timed semantic and phonemic fluency tasks to assess their verbal fluency. Diffusion MRI with probabilistic tractography was used to segment the bilateral cerebellar peduncles (CPs) and frontal aslant tract (FAT), previously associated with speech production in clinical populations. Our results demonstrate distinct patterns of white matter associations with different fluency components. Specifically, verbal fluency is associated with the right superior CP, whereas speaking rate is associated with the right middle CP and bilateral FAT. No association is found with articulation rate in these pathways, in contrast to previous findings in persons who stutter. Our findings support the contribution of the cerebellum to aspects of speech production that go beyond articulatory control, such as lexical access, pragmatic or syntactic generation. Further, we demonstrate that distinct cerebellar pathways dissociate different components of speech fluency in neurotypical speakers.

INTRODUCTION

Humans produce about 16,000 words every day, at an astounding speed of more than 150 words per minute (Amir, 2016; Mehl et al., 2007; Rodero, 2012). Such fast and fluent speech production depends upon complex interactions between motor, sensory and cognitive systems underpinning different aspects of speech production, such as articulatory control, phonological encoding, conceptual framing and lexical access (Hickok, 2012). Despite these interactions, most studies investigating speech fluency focus on either articulatory control or lexical access, but not both. Here, we combine the two perspectives to allow a comprehensive understanding of the neural pathways associated with fluent speech production in neurotypical adults.

Lexical access, including lexical search, selection, and retrieval, is typically measured using verbal fluency tasks. In these tasks, participants are asked to produce as many words as possible within 60 seconds under a specific criterion: words beginning with a certain letter (i.e., phonemic fluency) or a semantic category (i.e., semantic fluency). Verbal fluency is often assessed in clinical populations such as persons with aphasia (Bose et al., 2022), dementia (Libon et al., 2009), multiple sclerosis (Blecher et al., 2019), Parkinson's disease (Henry & Crawford, 2004), and more. Importantly, performance in the verbal fluency task is influenced by adequate word selection and avoidance of repetition. Therefore, these tasks are used to assess not only lexical knowledge, but also executive functions such as working memory and inhibition (Amunts et al., 2020; Shao et al., 2014). Indeed, verbal fluency is a central task in neuropsychological batteries that assess executive functions (Kramer et al., 2014; Shao et al., 2014).

Fluent speech production is also quantified using measures of speech rate. In contrast to the timed and highly constrained nature of verbal fluency tasks, speech rate measures, such as *Speaking rate* and *Articulation rate*, are based on a relatively naturalistic setting of spontaneous speech samples. Broadly, speech rate is calculated as the number of spoken units (syllables or words) produced within a time unit (second or minute). *Speaking rate* is measured across continuous segments of speech which may include pauses, repetitions, and revisions. Thus, it is considered a global measure of verbal output and language proficiency (Costello & Ingham, 1984; Howell et al., 1999). *Articulation rate*, on the other hand, is based only on fluent utterances after excluding any kind of disfluency, and thus considered a measure of articulatory motor control (Walker et al., 1992). Generally, speech rate (as quantified by both measures)

affects the speakers' intelligibility, fluency, and communication efficiency (Amir, 2016; Sturm & Seery, 2007). Measures of speech rate are typically used in the clinical assessment of various speech disorders, such as apraxia of speech (Kent & Rosenbek, 1983), dysarthria (Kent et al., 1987), and persistent developmental stuttering (Andrade et al., 2003).

Although speech fluency involves both lexical access and articulatory control, studies in the field tend to focus either on linguistic aspects of speech or on motor aspects of speech, but not both. In an attempt to bridge this gap, Hickok has recently suggested the Hierarchical State Feedback Control (HSFC) model of speech production (Hickok, 2012). This model synthesizes between psycholinguistic and motor control approaches and suggests an integrated brain circuitry of speech production. The current understanding of the brain circuits that control fluent speech production, however, stems largely from studies in patients. Hence, in the current study we wish to evaluate the different interpretations of speech fluency and evaluate the neural substrates that stand at the base of fluent speech production in neurotypical adults.

According to computational models of speech production, the cerebellum is a key node in different aspects of fluent speech production (Hickok, 2012; Tourville & Guenther, 2011). Indeed, patients with cerebellar lesions exhibit impaired verbal fluency abilities and significantly slower speaking rate and articulation rate compared to controls (Ackermann et al., 1992; Peterburs et al., 2010). Neuroimaging data point to a significant cerebellar activation during both verbal fluency tasks (Halari et al., 2006; Schlösser et al., 1998) and tasks that involve change in articulation rate (Riecker et al., 2005, 2006). Naturally, the involvement of the cerebellum in verbal fluency tasks could stem from the fact that fluency tasks use the articulatory system. Therefore, to make a functional segregation, the contribution of the cerebellum to each of these measures should be evaluated in the same participants.

Apart from the cerebellum, neural control of speech recruits a distributed cortical network (Hickok, 2012; Tourville & Guenther, 2011). The cortex and the cerebellum are structurally connected via long range white matter pathways which enable efficient communication of signals across considerable distance. As the exclusive bridge between the cerebellum and extra-cerebellar regions, the structural properties and organization of the cerebellar peduncles are important for understanding the neural basis of fluent speech production.

Cerebellar input and output information is carried by three major white matter pathways known as the cerebellar peduncles (CPs): the inferior cerebellar peduncle (ICP), the middle

cerebellar peduncle (MCP), and the superior cerebellar peduncle (SCP). The ICP is a cerebellar input pathway, feeding signals from the inferior olive and spinal cord into the cerebellar cortex (Perrini et al., 2013). The ICP was shown to be implicated in articulation rate among people with developmental stuttering. Developmental stuttering was previously associated with abnormalities in the microstructural properties of the bilateral ICP (Connally et al., 2014; but see Jossinger et al., 2021, 2022 for contradicting results). A recent study in young children who stutter showed that microstructural differences in the ICP emerge early in development (Johnson et al., 2022). In adults with developmental stuttering, but not in neurotypical speakers, the microstructural properties of the ICP was shown to be correlated with articulation rate (Jossinger et al., 2021; Kronfeld-Duenias et al., 2016).

The SCP is a major output pathway transmitting signals from the cerebellum into the contralateral cerebral cortex via the thalamus. The MCP is a major input pathway feeding signals from the cerebral cortex into the contralateral cerebellar cortex, decussating at the level of the pontine nucleus. Together, the SCP and MCP form the cerebro-cerebellar loop which allows transferring information from the cerebellum to the cerebral cortex and vice versa. Computational models of speech production hypothesize that the cerebro-cerebellar projections contribute to the feedforward control of speech by mapping between the desired speech sound and its appropriate articulatory gesture (Tourville & Guenther, 2011). Recent data show that the cerebro-cerebellar connectivity is also associated with speech-related cognitive demands, such as verbal working memory (Sobczak-Edmans et al., 2019) and story comprehension (Castellazzi et al., 2018). Functional MRI (fMRI) studies have shown that verbal fluency tasks cause a significant activation in the cerebellum, together with prefrontal and temporo-parietal areas (Gurd et al., 2002; Hubrich-Ungureanu et al., 2002; Schlösser et al., 1998). On this basis, cerebellar activity during verbal communication may reflect not only motor aspects of speech production, but also cognitive demands of word generation.

The potential involvement of the cerebro-cerebellar loop in the fluent production of speech is further supported by the anatomical connections found between the cerebellum and the prefrontal cortex (Kelly & Strick, 2003; Middleton & Strick, 1994; Palesi et al., 2017). Within the prefrontal cortex, feedforward control of speech involves the activation of the inferior frontal gyrus (IFG) and the supplementary motor area (SMA) (Hickok, 2012; Tourville & Guenther, 2011). The IFG and SMA were recently shown to be connected via the frontal aslant tract (FAT)

(Catani et al., 2012). To date, the involvement of the FAT in speech fluency was mainly studied in clinical populations. For example, Kronfeld-Duenias et al. (2016) showed that adults who stutter demonstrate abnormal microstructure within the FAT compared to fluent speakers. This structural difference was also accompanied by a correlation between the microstructural properties of the FAT and articulation rate, association which was not evident in fluent speakers. Interestingly, in patients with multiple sclerosis and in patients with chronic aphasia, the FAT was associated with verbal fluency measures (Blecher et al., 2019; Catani et al., 2013; Li et al., 2017).

In the current study, we evaluated the contribution of the CPs and the FAT to the different measures of speech fluency in neurotypical adults. Participants (N=45) underwent an unstructured interview to assess their natural speaking rate and articulation rate, and completed timed semantic and phonemic fluency tasks to assess their verbal fluency. Diffusion MRI data was measured in the same group of participants using a single-shell high angular resolution imaging (HARDI) sequence (Tuch et al., 2003). The automatic fiber segmentation and quantification (AFQ) package (Yeatman et al., 2012) was adapted in order to delineate the bilateral SCP and MCP as they decussate at the level of the inferior colliculi and pons, respectively. Microstructural properties were extracted from the CPs and the FAT, and entered into correlation analyses with measures of speech fluency. Based on computational models of speech production (Hickok, 2012; Tourville & Guenther, 2011), and on previous neuroimaging reports (Castellazzi et al., 2018; Gurd et al., 2002; Hubrich-Ungureanu et al., 2002; Schlösser et al., 1998b; Sobczak-Edmans et al., 2019), we expected that the microstructural properties of the cerebro-cerebellar loop (i.e., SCP and MCP) will be correlated with both articulatory and verbal aspects of speech production. Importantly, this analysis is still exploratory, due to the lack of prior data or modelling work relating each CP to specific language functionalities. Based on previous studies of structural connectivity in clinical populations (Blecher et al., 2019; Catani et al., 2013; Li et al., 2017), we hypothesized that the microstructural properties of the FAT will be associated with verbal fluency measures in the current sample of neurotypical adults. Lastly, based on our previous findings (Jossinger et al., 2021; Kronfeld-Duenias et al., 2016), neurotypical adults were not expected to show an association between articulation rate and the ICP or the FAT.

METHODS

Participants

Forty-five neurotypical adults (29 females; mean age 26.45 ± 3.72 years; Table 1) were recruited for this study. All the analyses reported here are completely new, but some data from this sample has been reported as part of a research project focusing on associations between well-known language pathways and word structure (Yablonski et al., 2021; Yablonski & Ben-Shachar, 2020). All participants were right handed as estimated by the Edinburgh handedness inventory (Oldfield, 1971; Table 1), and had no history of a diagnosed speech impairment, learning disability, or neurological condition. All participants were native Hebrew speakers who speak and read English as L2. One participant was referred to neurological follow-up due to an incidental finding, but otherwise had normal anatomical structure and diffusion values and was thus not excluded from analysis. Participants were paid 200 NIS for their participation. All participants signed a written informed consent before participating in the study. This study was approved by the Helsinki committee of the Sheba Medical Center, by the Institutional Review Board of Tel Aviv University, and by the Ethics committee of the Faculty of Humanities in Bar-Ilan University.

Table 1. Sample characteristics (N=45).

	mean	*SD*	*range*
Demographics			
Gender	16M/29F	--	--
Age (years)	26.45	3.72	[20.23, 34.87]
Education (years)	14.56	2.13	[12, 20]
Handedness	96.89	5.90	[80,100]
Speech rate			
Speaking rate (syllables/sec)	5.04	0.68	[3.49, 6.78]
Articulation rate (syllables/sec)	6.42	1.05	[4.57, 9.08]
Verbal fluency			
Phonemic fluency (Words/min)	43.78	9.83	[17, 68]
Semantic fluency (Words/min)	66.96	12.22	[46, 99]

Speech fluency assessment

Speaking task. Speaking rate and articulation rate were measured over audio recordings of an unstructured interview. The interview took place in a quiet room, and was simultaneously recorded with a noise-canceling microphone (Sennheiser PC21-II, Sennheiser Electronic Corporation, Berlin, Germany) and with a digital video camera (Sony HDR-CX405, Sony corporation of America, New York, NY, USA). Audio signals from the microphone were digitally recorded using Audacity (https://audacityteam.org/) on a mono channel with a sampling rate of 48 kHz (16 bit). The participant was asked to talk about a neutral topic (e.g., a recent travel experience, a movie, a book), for about 10 min. The experimenter (M.Y.) refrained from interrupting, asking open questions only when the participant was having difficulty finding a topic to talk about.

Speech rate measures. Two speech rate measures were calculated: Speaking rate and articulation rate. Both measures were calculated over the audio recordings of the unstructured interview. *Articulation rate* was calculated as the ratio between the total number of analyzed syllables and the time it took the participant to produce them (i.e., syllables/sec), after excluding disfluent utterances (Ambrose & Yairi, 1999; Amir, 2016; Amir & Grinfeld, 2011; Rochman & Amir, 2013). *Speaking rate* was calculated in the same way, on the entire speech segment without exclusions. For this purpose, two trained research assistants first transcribed each interview and annotated any disfluent epochs (mostly naturally occurring disfluencies, such as hesitations, repetitions, and revisions). An utterance was defined based on three criteria: (1) communicated an idea, (2) had a well-defined intonation contour, and (3) was grammatically complete. Overall, a fixed number of 50 utterances were used to calculate Speaking rate, and 12.8 ± 6.36 utterances were used to calculate articulation rate.

Verbal fluency tasks. Normed Hebrew versions of the phonemic and semantic fluency tasks were implemented (Kavé, 2006; Kavé & Knafo-Noam, 2015). Participants were asked to produce as many words as possible within 1 minute according to a criterion: words beginning with a certain letter (phonemic fluency tasks) or a semantic category (sematic fluency tasks). Each task was repeated 3 times with different criteria. For the Phonemic fluency task, participants were asked to produce words that begin with the letters Bet (/b/), Gimel (/g/), and Shin (/ʃ/ or /s/). For the Semantic fluency task, participants were asked to produce words that

belong to the categories animals, fruits and vegetables, and vehicles. The administration order of the tasks and the different items within each task was kept constant across participants, starting with the phonemic fluency task and followed by the semantic fluency task. The experimenter (M.Y.) read each criterion aloud, and participants' oral responses were recorded and transcribed offline.

Verbal fluency measures. First, responses in both tasks were screened according to the guidelines described in Kavé & Knafo-Noam (2015). Accordingly, repetitions and erroneous responses were removed. For example, in the semantic fluency task, names of subcategories (e.g., birds) were not counted if the participant also produced specific exemplars within the subcategory (e.g., raven, pigeon). The total number of correct unique responses was coded per criterion and summed across the three criteria within each task. We also calculated a standardized verbal fluency score based on age-appropriate Hebrew norms (Kavé & Knafo-Noam, 2015). The analysis of standardized verbal fluency scores in the current sample is reported in a previous paper (Yablonski et al., 2021). Note, however, that this previous paper did not examine the associations between verbal fluency measures and the CPs, which is the focus of the current study.

Behavioral inter-correlation analysis

Correlations between speech fluency components were calculated using the open-source R environment for statistical analysis (R Core Team, 2013). Specifically, we calculated Spearman's correlations between speaking rate, articulation rate, phonemic fluency, and semantic fluency, resulting in an inter-correlation matrix of 6 correlations overall. To account for multiple comparisons, we controlled the false discovery rate (FDR) at a level of 5% (Benjamini & Hochberg, 1995).

White matter analysis

MRI data acquisition

MRI scans were conducted on a 3T Siemens Magnetom Prisma scanner at the Strauss Center for Computational Neuroimaging at Tel Aviv University, with a 64-channel head coil. The MRI

protocol included standard anatomical and diffusion imaging sequences, as detailed below. Functional MRI scans were also included in the scanning protocol but are not reported here.

T1 image acquisition. High-resolution T1-weighted anatomical images were acquired using a magnetization prepared rapid acquisition gradient echo (MPRAGE) protocol (TR=2.53 s, TE=2.99 ms, flip angle=7º, 1 mm thick slices, matrix size: 224 ×224 ×176, voxel size: 1 ×1 ×1mm).

Diffusion weighted image acquisition. A standard diffusion MRI (dMRI) protocol was applied by means of a single-shot spin-echo diffusion-weighted echo-planar imaging (DW-EPI) sequence (86 axial slices, each 1.7 mm thick, no gap; FOV = 204 ×204 mm, image matrix size = 120 ×120 providing a cubic resolution of 1.7 ×1.7 ×1.7 mm, TR = 4000 ms, TE = 58 ms). Sixty-four diffusion-weighted volumes (b = 1000 s/mm^2) and three reference volumes (b = 0 s/mm^2) were acquired using a standard diffusion direction matrix. Multiband acceleration was used with slice acceleration factor of 2. Total acquisition time for the dMRI sequence was 4:48 min.

MRI data analysis

Software. Data analysis was conducted using Matlab 2012b (The Mathworks, Natick, MA). Data preprocessing was obtained using the open source 'mrDiffusion' package (https://github.com/vistalab/vistasoft/tree/master/mrDiffusion). Constrained spherical deconvolution (CSD) diffusion model was calculated using the 'mrTrix3' toolbox (https://www.mrtrix.org/; Tournier et al., 2019). Tract identification and quantification were executed with the automatic fiber segmentation and quantification (AFQ) toolkit (https://github.com/yeatmanlab/AFQ; Yeatman et al., 2012). Individual tracts were visually inspected using Quench, an interactive 3D visualization tool (http://web.stanford.edu/group/vista/cgi-bin/wiki/index.php/QUENCH; Akers, 2006).

Data preprocessing. Preprocessing was implemented in the native space of each individual, following a published pipeline (Yablonski et al., 2021). This pipeline included several steps: (1) Alignment of the T1 images to the anterior commissure –posterior commissure (AC-PC) orientation; (2) Motion- and eddy-current correction of DW-EPI data (Rohde et al., 2004); (3) Registration of the diffusion weighted volumes to the averaged non-diffusion weighted volumes (b0); (4) Registration of the mean b0 image to the T1 image using a rigid body mutual

information maximization algorithm (implemented in SPM8; Wells et al., 1996); (5) Applying the combined transform resulting from motion correction, eddy-current correction and anatomical alignment to the raw diffusion data; (6) Adjusting the table of gradient directions to fit the resampled diffusion data (Leemans & Jones, 2009).

At the voxel level, the diffusion data was modeled twice, once with the tensor model and once with the constrained spherical deconvolution (CSD) model. Diffusion tensors were used to calculate, within each voxel, the commonly used diffusion metrics (e.g., fractional anisotropy, etc.), which were later used for the statistical analysis. Tensor modeling was carried out using 'mrDiffusion'. Tensors were fit to the registered diffusion data using a robust least-square algorithm (RESTORE), which removes outliers at the tensor estimation step (Chang et al., 2005). Then, using tensor decomposition, we extracted the three eigenvalues and eigenvectors of the tensor, and calculated, within each voxel, fractional anisotropy (FA) and mean diffusivity (MD). Specifically, FA was calculated as the normalized standard deviation of the eigenvalues, and MD was calculated as the average of the three eigenvalues (Basser & Pierpaoli, 1996).

As the tensor model is notoriously known for its inability to account for multiple orientations within the same voxel (Jones et al., 2013), our individual tractograms were generated based on the CSD model. The CSD model estimates the fiber orientation distribution (FOD) within each voxel based on the spherical deconvolution between the diffusion weighted signal and an estimation of the diffusion response function (Tournier et al., 2004, 2007). To calculate the CSD model we used the 'mrTrix' toolbox (Tournier et al., 2019). First, to estimate the response function we used the *dhollander* algorithm (implemented within the *dwi2response* function). This algorithm estimates the response functions for white matter, gray matter, and cortico-spinal fluid (CSF), separately, based on single-shell diffusion data. Next, to estimate the FOD, we applied constrained spherical deconvolution with up to eight spherical harmonics (lmax = 8) on the responses estimated within the white matter and the CSF. This step was carried out by the *msmt_csd* algorithm (implemented within the *dwi2fod* function) (Jeurissen et al., 2014). Lastly, the FODs were used to generate individual tractograms using probabilistic tractography, as explained below.

Fiber tractography. Individual tractograms were generated using probabilistic whole brain tractography, with the iFOD2 tracking algorithm (implemented in the mrTrix3 function *tckgen*).

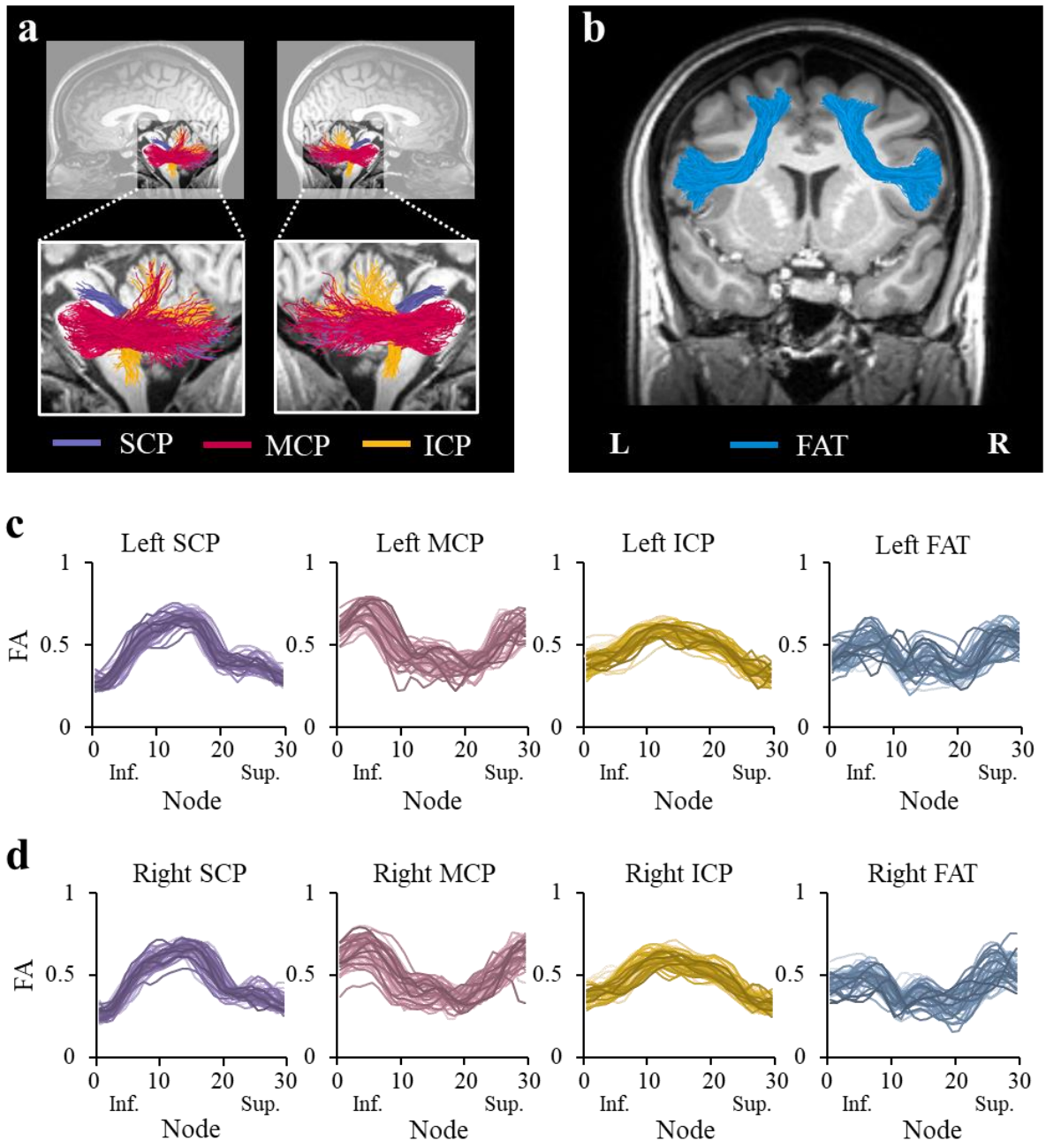

Figure 1. Tracts of interest. a) Shown are the left and right cerebellar peduncles identified in a single participant (female, 34), overlaid on a T1 image. The cerebellar tracts identified are the superior cerebellar peduncle (SCP; purple), middle cerebellar peduncle (MCP; magenta), and the inferior cerebellar peduncle (ICP; yellow). b) Shown are the left and right frontal aslant tract (FAT; blue) identified in a single participant (female, 24), overlaid on a T1 image. c-d) Individual tract profiles show FA values at 30 equidistant nodes along the core of the left (c) and right (d) tracts of interest. Each subject is represented by a single line (N=45). Abbreviations: SCP – superior cerebellar peduncle; MCP – middle cerebellar peduncle; ICP – inferior cerebellar peduncle; FAT – frontal aslant tract; L – left; R – right; Inf. – inferior; Sup. – superior.

As a first step, a whole brain white matter mask was generated from each participant's structural T1 image. This procedure was done using the *5ttgen* script, utilizing FSL tools to perform whole brain segmentation (Smith et al., 2004). The tracking was initialized from 500,000 random seeds within the white matter mask, and was restricted with the following parameters: (1) FOD amplitude threshold of 0.1; (2) 45º maximum angle between successive steps; (3) 0.85 mm step size; (4) streamline length between 50mm to 200mm. Streamlines that extended beyond the white matter mask were truncated. The resulting whole brain tractograms were then subjected to the automatic tract segmentation procedure.

Tract identification and segmentation. In each individual's native space, we identified the bilateral CPs and the bilateral FAT (Figure 1). We targeted these tracts based on previous studies in clinical populations, directly linking the CPs (Figure 1a) and the FAT (Figure 1b) to speech fluency (Blecher et al., 2019; Catani et al., 2013; Connally et al., 2014; Jossinger et al., 2021; Kronfeld-Duenias et al., 2016; Li et al., 2017), and based on theoretical models of speech production (Hickok, 2012; Tourville & Guenther, 2011). Automatic segmentation of the tracts was carried out using AFQ. This method utilizes a multiple-ROI approach in which the tractograms are intersected with pre-defined ROIs using logical operations (Figure S1). In accordance with this method, the ROIs are universally defined on a template (Figure S1a), and then back-transformed to the participant's native space using a non-linear transformation (Figure S1b). The individual ROIs are intersected with the tractogram (Figure S1c) to isolate the tracts of interest (Figure S1d). To identify the CPs we propose a new protocol which is based on several previous studies (Bruckert et al., 2019; Palesi et al., 2015, 2017). To identify the bilateral FAT, we used the protocol described in Kronfeld-Duenias et al. (2016), which is implemented in AFQ (publicly available at https://github.com/yeatmanlab/AFQ/tree/master/aslant).

Automatic segmentation of the CPs was recently introduced by Bruckert et al. (2019). This approach, however, delineates only the inferior parts of the SCP and MCP, before they decussate to the contralateral cerebral hemisphere. For this reason, the methods introduced in Bruckert et al. (2019) are better suited to delineate the CPs based on deterministic tractography, where fibers are less likely to decussate. On the other hand, probabilistic tractography approaches coupled with CSD modeling are more successful in following the CPs as they decussate. In order to segment the resulting tracts automatically, we revised the AFQ protocol including additional ROIs (see Fig. S2 and Table S1 for detailed MNI coordinates of the ROIs).

The new set of ROIs used to identify the CPs were defined on the Montreal Neurological Institute (MNI) template (ICBM 2009a Nonlinear Asymmetric template; Fonov et al., 2011). For the SCP, a new ROI (SCP_superior_prob) was defined on an axial slice at the level of z = -10, encompassing a rectangle around the red nucleus (Oishi et al., 2009; Palesi et al., 2015). The SCP was then segmented using the newly defined ROI together with the previous SCP-ROIs described by Bruckert et al. (2019) (Figure S2a). For the MCP, a new ROI (MCP_superior_prob) was defined as a parallelogram on an axial slice at the level of z = -16, including all the voxels occupied by the cerebral peduncle (Oishi et al., 2009; Palesi et al., 2017). The MCP was then segmented using the newly defined ROI together with the previous MCP-ROI introduced by Bruckert et al. (2019) (Figure S2b). For the ICP, a new inferior ROI (ICP_inferior_prob) was defined to avoid fibers that enter the pons. The ICP was then segmented using the newly defined ROI together with the previous ICP-ROI introduced by Bruckert et al. (2019) (Figure S2c).

The resulting tracts were cleaned automatically using a statistical outlier rejection algorithm implemented in AFQ. For the cleaning procedure of the SCP, MCP and FAT, fibers were considered outliers if they were longer than 4 standard deviations from the mean fiber length and spatially deviated more than 4 standard deviations from the core of the tract. For the ICP, a relatively short tract, the length criterion was changed as previously done in (Bruckert et al., 2019,) such that fibers longer than 1 standard deviations from the mean fiber length were removed. The tracts are shown in Fig. S3 in 3 representative subjects.

Brain-behavior correlation analysis

The analyses were restricted to the core segment of each tract, enclosed between the two waypoint-ROIs (Figure S2). This approach eliminates the extreme segments of the tracts which are highly variable between participants.

Mean-tract correlations. Associations between diffusivity values and speech fluency measures were assessed using two-tailed Spearman's rank-order correlations. As a first step, we calculated for each participant and each tract the average FA and average MD values across the core of the tract (i.e., tract-FA and tract-MD, respectively). Then, we assessed the simple correlations between tract-FA and speech fluency measures. We controlled for multiple comparisons across 8 tracts setting the FDR at a level of 5% (Benjamini & Hochberg, 1995). A similar analysis was conducted on tract-MD values. Separate analyses were conducted for each behavioral measure (Xie et al., 2011).

Along-tract correlations. It is well documented that diffusivity values vary significantly along the tract (Yeatman et al., 2011, 2012). This is also true for the CPs and the FAT, as shown in Figure 1c-d and Figure S4. We therefore applied a second analysis, assessing two-tailed Spearman's correlations between speech fluency measures and diffusivity values at 30 equidistant locations along the core of the tract (Kruper et al., 2021). To account for multiple comparisons, significance was corrected using a non-parametric permutation test, controlling the family-wise error (FWE) at a corrected alpha value of 0.05 (Nichols & Holmes, 2002). Clusters were considered significant if they satisfied two criteria: (1) each node within the cluster was significantly correlated with speech fluency at a level of alpha = 0.05 (uncorrected), and (2) the number of adjacent nodes composing the cluster should have been larger than a critical size, determined by the permutation algorithm (Nichols & Holmes, 2002; Yeatman et al., 2012). FWE correction was applied across the 30 nodes within each tract, with no further correction across tracts, behavioral measures, or diffusion metrics (see e.g., Yablonski et al., 2021, Yeatman et al., 2012 for similar approach).

Partial correlation. To assess the specificity of associations and dissociate between tracts mediating lexical or articulatory components of speech fluency, significant associations were followed up by Spearman's partial correlations. For example, associations with speaking rate were followed up with partial correlation analyses that held constant the contribution of articulation rate.

RESULTS

Behavioral correlations

A correlation matrix of the four speech production measures (Figure 2a, Table S2) demonstrated significant correlations between the Speaking- and Articulation- rates ($r = 0.599$, $p < 10^{-4}$), and between the semantic- and phonemic- fluency scores ($r = 0.548$, $p < 10^{-4}$; both correlations were significant when controlling the FDR at $q<0.05$). However, non-significant correlations were found between the verbal fluency measures and the speech rate measures ($p > 0.06$, uncorrected). Articulation rate was higher than speaking rate in all participants (Figure 2b;

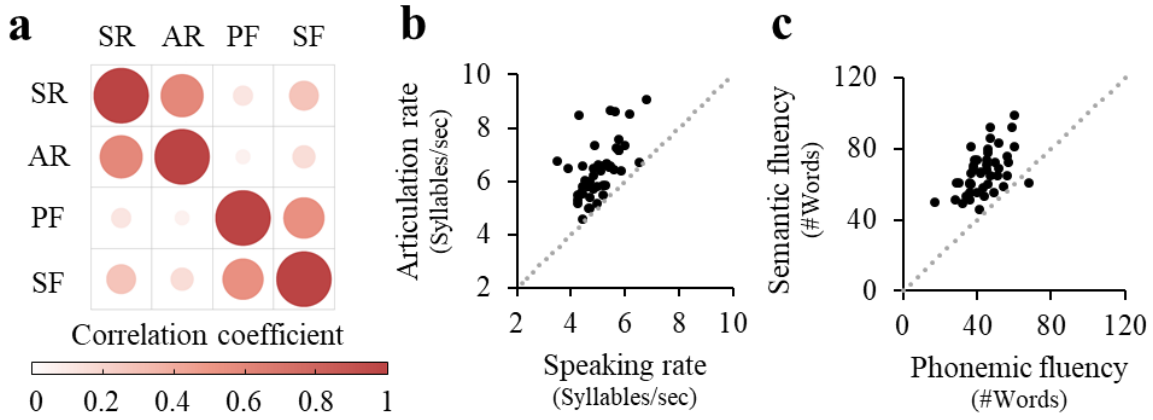

Figure 2. Behavioral dissociation between verbal fluency measures and speech rate measures. a) Correlation matrix depicting two-tailed Spearman's correlation coefficients between the four fluency measures calculated: speaking rate (SR), articulation rate (AR), phonemic fluency (PF), and semantic fluency (SF). The color saturation and size of the circles are proportional to the correlation coefficients. Panels (b) and (c) depict the associations between speaking and articulation rate (b), and between phonemic and semantic fluency (c). Both correlations were significant after controlling the FDR across all behavioral measures at $q < 0.05$. Dashed lines delineate $y=x$. Abbreviations: SR – speaking rate; AR – articulation rate; PF – phonemic fluency; SF – semantic fluency.

consistent with (Amir, 2016). Semantic fluency scores were higher than phonemic fluency scores in 44/45 participants (Figure 2c; consistent with (Kavé, 2005)). Repeating this analysis with age standardized scores (Kavé & Knafo-Noam, 2015) generated a similar pattern of results (see Table S3).

Tract identification

The bilateral cerebellar peduncles and the bilateral frontal aslant tract were successfully identified in all 45 participants (Figure 1). A qualitative examination of the tractograms (Figure 1a-b) and the individual tract profiles (Figure 1c-d) verified that the tracts were accurately segmented and provided consistently shaped profiles in all individuals (see Figure S3 for tract reconstruction in 3 representative participants).

Speech fluency associations within the cerebellar peduncles

To examine the relationships between speech fluency and the microstructural properties of the cerebellar peduncles in neurotypical adults, Spearman's correlations were first calculated between the four measures of speech fluency (speaking rate, articulation rate, phonemic fluency, and semantic fluency) and mean tract diffusivities (tract-FA and tract-MD; see *Methods*) within

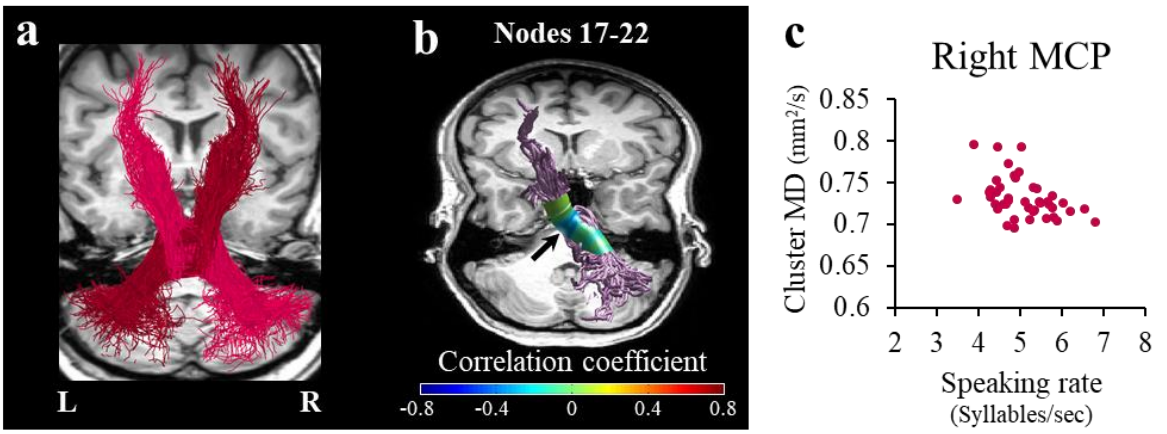

Figure 3. Mean diffusivity in the right middle cerebellar peduncle correlates with speaking rate. a) The full trajectories of the right MCP (magenta) and the left MCP (burgundy) are shown in a representative subject (female, 27). b) Two-tailed Spearman's correlation coefficients are visualized in 30 nodes along the core of the right MCP. The black arrow denotes the location of the significant cluster of nodes (nodes 17-22, $p<0.05$, family-wise error corrected across 30 nodes). c) A scatter plot showing the association between speaking rate and the averaged MD in the significant cluster of nodes within the right MCP. Abbreviations: MCP – middle cerebellar peduncle; MD – mean diffusivity; L – left; R – right.

each of the cerebellar peduncles. No significant correlations were detected between speech fluency and mean tract diffusivities in the cerebellar peduncles. Calculating the correlation for the *age-standardized* verbal fluency measures did not change these results. See Tables S4-S5 for a detailed list of correlation values.

To achieve enhanced sensitivity for detecting localized brain-behavior correlations, we examined the relationships between speech fluency and local diffusivity values, node-by-node, along the trajectory of each cerebellar peduncle (see *Methods*). This analysis revealed a dissociation in the pattern of correlations within the cerebellar peduncles, such that MD within the right MCP was significantly correlated with speaking rate ($r = -0.447$, $p < 0.05$, nodes 17-22, FWE corrected across 30 nodes; Figure 3), whereas FA within the right SCP was significantly correlated with phonemic fluency ($r = 0.431$, $p < 0.05$, nodes 19-24, FWE corrected across 30 nodes; Figure 4). Note that both significant clusters were detected in the vicinity of the decussation. We address this point in the discussion.

Importantly, these correlations remained significant when calculating partial correlations, such that the correlation between the right MCP and speaking rate was not driven by phonemic fluency ($r = -0.451$, $p = 0.002$), and the correlation between the right SCP and phonemic fluency was not driven by speaking rate ($r = 0.438$, $p = 0.003$). Moreover, controlling for the contribution

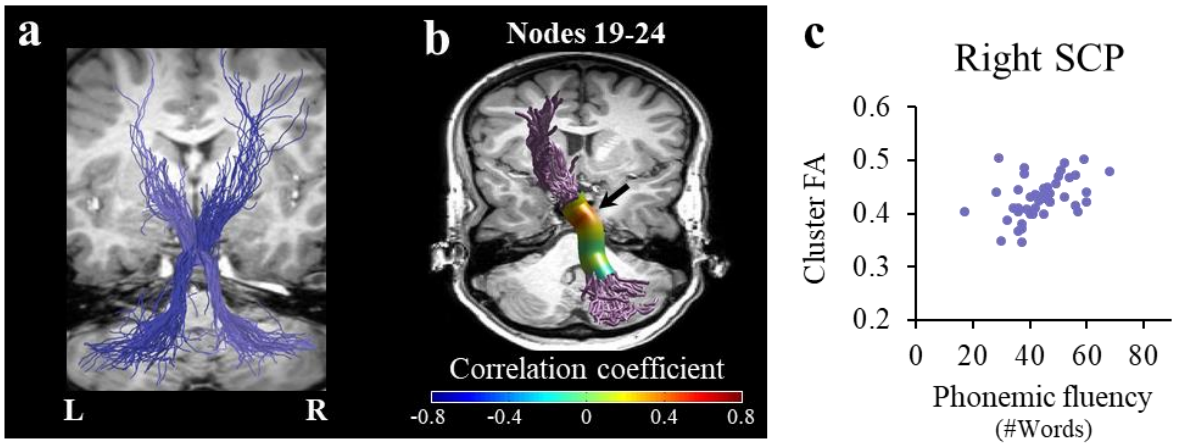

Figure 4. Fractional anisotropy in the right superior cerebellar peduncle correlates with phonemic fluency. a) The full trajectories of the right SCP (light purple) and the left SCP (dark purple) are shown in a representative subject (female, 27). b) Two-tailed Spearman's correlation coefficients are visualized in 30 nodes across the core of the right SCP. The black arrow denotes the location of the significant cluster of nodes (nodes 19-24, $p<0.05$, family-wise error corrected across 30 nodes).. c) The scatter plot shows the association between phonemic fluency and mean FA in the significant cluster of nodes within the right SCP. Abbreviations: SCP – superior cerebellar peduncle; FA – fractional anisotropy; L – left; R – right.

of articulation rate did not change these effects (Right MCP: $r = -0.477$, $p = 0.001$; Right SCP: $r = 0.442$, $p = 0.003$).

No additional significant correlations were found between the microstructural properties of the cerebellar peduncles and speech fluency measures (Table S4). Importantly, in line with a previous report (Jossinger et al., 2021), we did not find significant correlations between articulation rate and diffusivities within the left ICP of neurotypical adults ($p > 0.5$; Figure 5). Notice that, because there was no significant cluster of nodes in the ICP, the scatter plot in Figure 5c depicts tract-FA (rather than cluster FA) against articulation rate.

Speech fluency associations within the bilateral frontal aslant tracts

To examine the relationships between speech fluency and the microstructural properties of the FAT in neurotypical adults, Spearman's correlations were first calculated between the four measures of speech fluency (speaking rate, articulation rate, phonemic fluency, and semantic fluency) and tract diffusivities (tract-FA and tract-MD; see *Methods*) within the bilateral FAT (Table S4). This analysis revealed that tract diffusivities within the bilateral FAT were

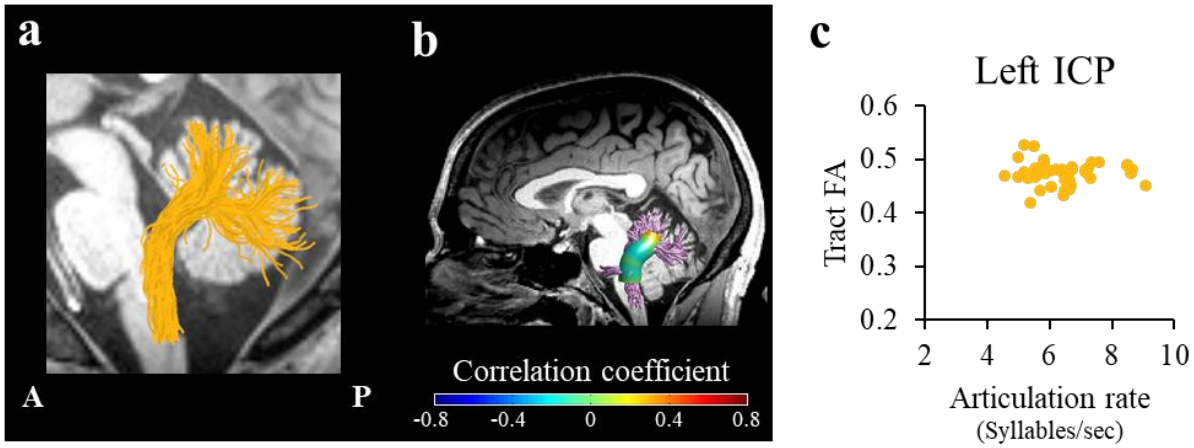

Figure 5. No correlation between the FA in left inferior cerebellar peduncle and articulation rate. a) The trajectory of the left ICP (yellow) is shown in a representative subject (female, 24). b) Two-tailed Spearman's correlation coefficients are visualized in 30 nodes across the core of the left ICP. c) Articulation rate is plotted, for each participant, against tract-FA (the mean FA across 30 nodes in the left ICP, See Methods). Abbreviations: ICP – inferior cerebellar peduncle; FA – fractional anisotropy; A – anterior; P – posterior.

significantly correlated with speaking rate (Figure 6a-c). Specifically, speaking rate was positively correlated with tract-FA within the left FAT ($r = 0.459$, $p < 0.002$; Figure 6a) and with tract-FA within the right FAT ($r = 0.466$, $p < 0.002$; Figure 6b) (both correlations were significant when controlling the FDR across 8 tracts at $q<0.05$). In both cases, neurotypical adults who speak faster have higher FA within their left and right FAT. In line with a previous report (Kronfeld-Duenias et al., 2016) no significant correlations were found between tract-FA within the bilateral FAT and articulation rate ($p > 0.1$; Figure 6d-f). Moreover, the correlations between the bilateral FAT and speaking rate remained significant when calculating partial correlations, controlling for the effect of articulation rate (Left FAT: $r = 0.465$, $p = 0.0014$; right FAT: $r = 0.488$, $p = 0.0007$). Fisher's Z test for dependent samples confirmed that the correlations between tract-FA and speaking rate differed significantly from the correlations with articulation rate (left FAT: Fisher's $Z = 2.396$, $p <0.009$; right FAT: Fisher's $Z = 2.605$, $p < 0.006$). See Tables S4-S5 for detailed correlation values between tract-FA and tract-MD values of the FAT and all speech fluency measures.

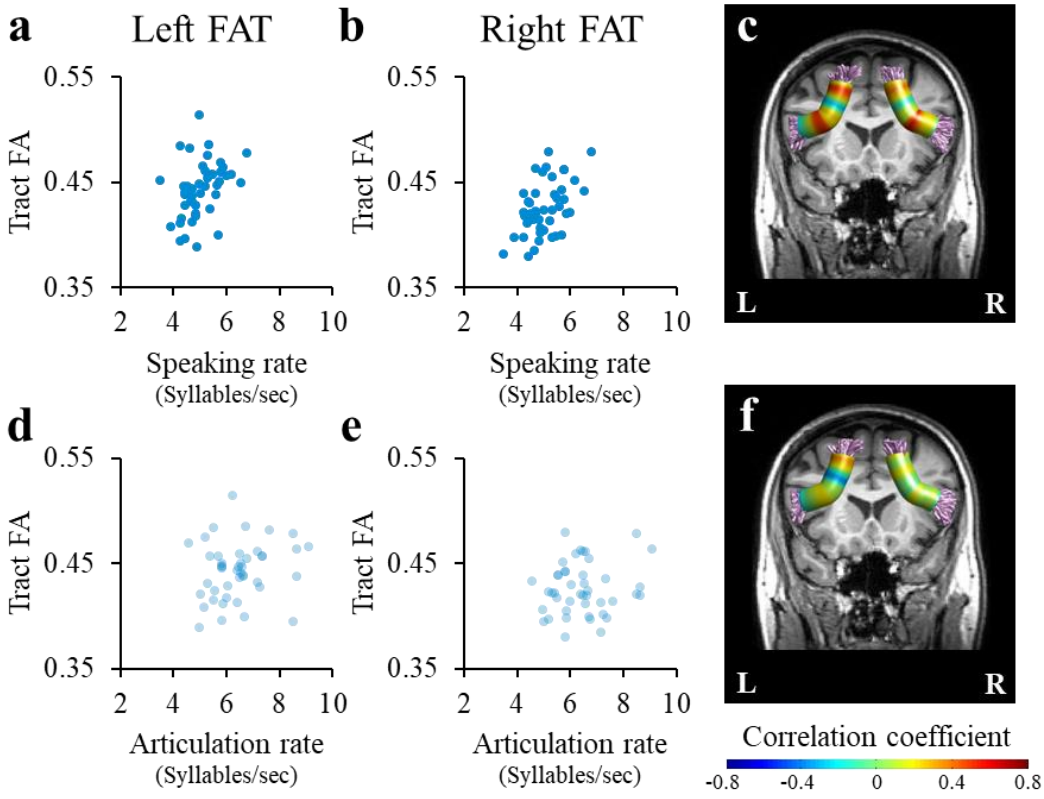

Figure 6. The bilateral frontal aslant tract is associated with speaking rate, but not with articulation rate. Scatter plots show the association between the number of syllables per second and tract-FA within the left FAT (a, d) and the right FAT (b, e). Tract-FA in the left and right FAT significantly correlated with speaking rate (blue; a-b, $q<0.05$, FDR corrected across all tracts), but not with articulation rate (light blue; d-e). For completeness, Spearman's correlation coefficients between FA and speaking rate, and between FA and articulation rate are visualized in 30 nodes along the left and right FAT (panels c and f, respectively). The correlations along the tracts did not pass FWE correction for 30 nodes. Abbreviations: FAT – frontal aslant tract; FA – fractional anisotropy; L – left; R – right.

For completeness, we also calculated the correlations with speech fluency measures along the trajectory of the bilateral FAT (see Fig. 6c for Speaking rate and 6f for Articulation rate). In line with tract-FA results (6a-b), several nodes showed positive local correlations with Speaking rate (Fig. 6c). However, these associations did not survive the FWE correction. Significant negative correlation was detected between speaking rate and MD within the right FAT (nodes 10-24; $r = -0.425$, $p < 0.05$ FWE correction across 30 nodes; Figure S4). This correlation remained significant when calculating partial correlation, controlling for the effect of articulation rate ($r = -0.325$, $p = 0.03$). No other significant correlations were found between diffusivities within the bilateral FAT and speech fluency measures (Table S4).

DISCUSSION

The goal of the current study was to evaluate the contribution of the CPs and the FAT to the fluent production of speech in neurotypical adults. Our findings demonstrate that the cerebellar peduncles dissociate between different speech fluency measures, such that the right MCP was associated with speaking rate while the right SCP was associated with phonemic fluency. These correlations were not driven by articulation rate. Further, we found that the bilateral FAT is also associated with speaking rate, but not with articulation rate. These findings shed light on the functional contributions of distinct subsystems involved in speech production. We discuss the findings concerning different aspects of speech fluency as they relate to the CPs and the FAT in the following sections.

Dissociation between verbal fluency and speech rate measures

The production of fast and fluent speech requires interaction between several processes, including high-level linguistic components, such as lexical access and phonological encoding, and motor components which are crucial for articulatory control. In the current study we assessed these different components by using different types of tasks that require overt production of speech: verbal fluency tasks and an unstructured interview. Our data show a behavioral dissociation between verbal fluency measures and speech rate measures (Figure 2). Moreover, we found that specific fluency measures mapped unto different white matter tracts. Together, these findings suggest that different fluency measures may reflect different aspects of speech production.

Task differences

The tasks we used to evaluate speech fluency differ in several aspects. First, an unstructured interview is a relatively naturalistic setting of speech production, while verbal fluency tasks measure speech production in a more artificial way. Second, producing a free narrative involves conceptualizing the message and projecting a syntactic structure, while a verbal fluency task elicits a list of words, mostly unconnected nouns, based on a predetermined criterion. Third, each task may involve different cognitive demands beyond speech production. For example, verbal fluency tasks require the use of executive functions such as response selection, the inhibition of irrelevant responses, and more (Friedman et al., 1998; Kramer et al., 2014). Spontaneously speaking during an unstructured interview, on the other hand, may be effected by the social and

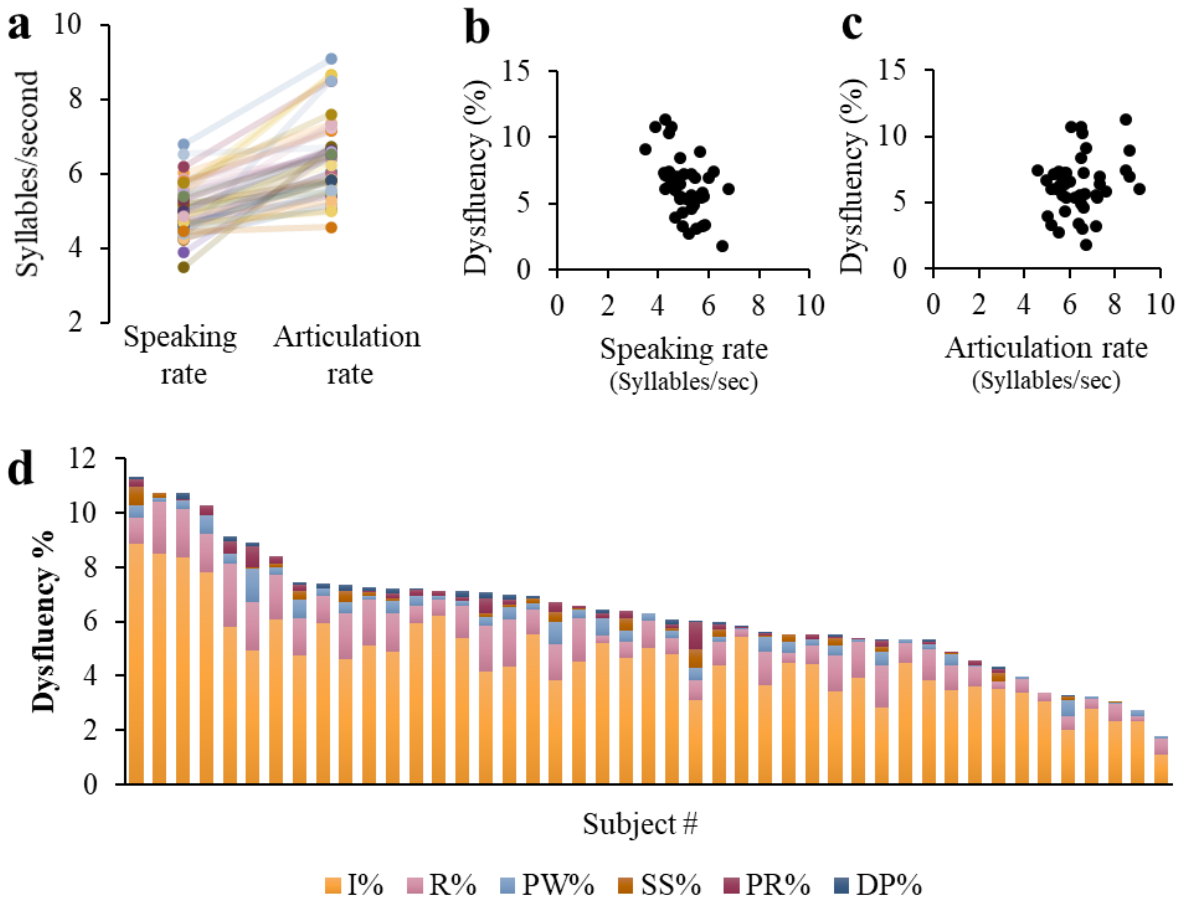

Figure 7. Analysis of individual speaking rate. (a) Individual speaking rates and articulation rates. Each line represents a single participant. In all participants, speaking rate is slower compared to articulation rate. (b-c) Speaking rate, but not articulation rate, is significantly associated with the percent of dysfluencies (r=-0.51, p = 0.0003 compared with r = 0.09, p = 0.56), such that slower speakers demonstrate more dysfluencies while they speak. (d) Distribution of dysfluencies by type. In our sample of neurotypical speakers, most dysfluencies included interjections (I%; e.g., "um") and revisions (R%; e.g., "so I was, we were…"). Other dysfluencies that occurred at much lower rates were part-word repetitions (PW%; e.g., "In, in.."), stuttered syllables (SS%; e.g., "The, the.."), phrase repetitions (PR%; e.g., "..because the flight was… the flight was"), and dysrhythmic phonation (DP%; e.g., "looooooves).

emotional state of the speaker (Amir, 2016). The extent to which each of the two speech fluency tasks used in this study relies on other cognitive functions, which are not speech-related, remains to be studied directly in future studies.

What does speaking rate actually measure?

Despite the considerable correlation between articulation rate and speaking rate (Figure 2b), the two metrics are thought to represent different aspects of speech production. Speaking rate, which is calculated over continuous segments of speech, including disfluencies of various sources, is considered a global measure of verbal output and language proficiency (Costello & Ingham, 1984). Articulation rate, in contrast, is calculated over the same speech samples but after excluding disfluent segments, thus thought to reduce linguistic effects and to represent articulatory motor control (Walker et al., 1992).

To better understand the sources of the differences between speaking and articulation rates, we conducted a more elaborate analysis of the individual speech segments, as described in Figure 7. As expected, in all participants, speaking rate is slower compared to articulation rate (Figure 7a). This difference may reflect naturally occurring disfluencies, which are included in the calculation of speaking rate, not articulation rate. In line with this view, speaking rate, but not articulation rate, is negatively correlated with the frequency of dysfluencies, such that slower speakers demonstrate more dysfluencies (compare Figure 7b and 7c). In our sample of neurotypical adults, the vast majority of dysfluencies included interjections (e.g., “um”) and revisions (e.g., “so I was, we were…”) (see Figure 7d). Such naturally occurring dysfluencies are commonly observed in neurotypical speakers and may reflect difficulties in formulating the message at different levels, e.g., the conceptual, syntactic or pragmatic levels.

Cerebellar internal models of speech and language

The cerebellum has long been viewed as a motor control structure. Over the past two decades, however, evidence points to a more general role for the cerebellum in the modulation of higher-level cognitive processes (Schmahmann, 2010). Our findings support this view by showing that the white matter pathways that connect the cerebellum to the cerebrum are important for the modulation of both speaking rate and phonemic fluency. Importantly, these correlations remain significant after we partial out the effect of articulation rate, a proxy for motor control. Therefore, the selective association patterns highlight the unique contribution of the cerebellum to linguistic, rather than motor components of speech, in neurotypical adults.

Cerebellar internal models

Studies focusing on the cerebellar computations postulate that it encodes "internal models", corresponding to the neural representations that we generate for the external world (Ito, 2008; Kawato, 1999; Shadmehr & Krakauer, 2008; Wolpert et al., 1998). This concept developed from contemporary theories of motor control, arguing that cerebellar internal models capture the causal relationships between a voluntary movement and its consequence. Internal models are used to predict the outcome of an action before the arrival of the actual sensory feedback from the environment. This mechanism is often used to explain how fast and coordinated movements can be carried out accurately, regardless of the slow nature of sensory feedback loops (Shadmehr & Krakauer, 2008; Wolpert et al., 1998). Indeed, current models of speech production argue that cerebellar internal models are used to transform motor-to-sensory information which is crucial for articulation, thus enabling fast and fluent production of speech (Guenther, 2006; Hickok, 2012).

Internal models of language in the cerebellum

The accumulative evidence implicating the cerebellum in high-level cognitive functions raises the possibility that cerebellar internal models are utilized to simulate mental representations, similarly to the manner in which they operate on motor behaviors (Ito, 2008). With respect to language processing, cerebellar internal models are hypothesized to store memories of sequential linguistic events, such as phonological, semantic and syntactic sequences, which are used to predict upcoming linguistic events during speech comprehension (Argyropoulos, 2016). By showing an association between the cerebero-cerebellar pathways and speech production, we may speculate that the cerebellum functions not only as an internal model during speech comprehension but may also contribute to prediction of linguistic elements during speech production.

Cerebro-cerebellar pathways mediate speech fluency in neurotypical adults

The hypotheses regarding the involvement of the cerebellum in cognition and language are largely based on the anatomical connections between the cerebellum and the cerebral cortex. In the late 1900's it was suggested that in humans, the increased size of the cerebellum and cerebral cortex led to the formation of new cerebro-cerebellar pathways that may contribute to high-level functions such as language (Leiner, 2010; Leiner et al., 1986). Connections between the

cerebellum and the prefrontal cortex were indeed traced in both monkeys (Middleton & Strick, 1994) and humans (Palesi et al., 2015, 2017). Recently, the cerebro-cerebellar pathways were implicated in various reading tasks that require overt production of speech (Bruckert et al., 2020; Travis et al., 2015). This is the first study, however, that shows a direct link between the microstructural properties of the cerebro-cerebellar pathways and speech fluency that goes beyond articulation, providing an anatomical and functional support to the hypotheses made in the 1980's (Leiner et al., 1986) .

The cerebro-cerebellar pathways dissociate between speech fluency measures

Our results point to distinct patterns of association between speech fluency measures and the microstructural properties of the cerebro-cerebellar pathways. Specifically, we found that the right SCP is associated with phonemic fluency (but not with speaking rate, see Figure 4 and accompanying text), while the right MCP is associated with speaking rate (but not with phonemic fluency, see Figure 3 and accompanying text). The difference in the functionalities associated with each peduncle is in line with the difference in the type of signals conveyed by each: the SCP is mainly an output pathway, transmitting signals from the cerebellar deep nuclei into the contralateral cerebral hemisphere, while the MCP is mainly an input pathway, feeding signals from the cerebral cortex into the contralateral cerebellar hemisphere. We may speculate that the involvement of the right SCP in phonemic fluency reflects the retrieval of phonological sequences from the cerebellar internal model, while the involvement of the right MCP in spontaneous speaking rate reflects the evaluation of the linguistic content against its internal representation. Future neurophysiological investigations will be essential to directly test this interpretation.

Functional lateralization within the cerebellum

Our findings demonstrate a functional lateralization within the cerebellum, by associating linguistic aspects of speech production with microstructural properties of the right SCP and right MCP. The concept of the "lateralized linguistic cerebellum", implicating the right cerebellar hemisphere in linguistic operations (Marien et al., 2001), has been well established in previous studies. For example, tasks that require lexical access and word retrieval were shown to activate the inferior lateral part of the right cerebellar hemisphere in neurotypical adults (Petersen et al., 1988, 1989). Further, patients with damage to the right cerebellar hemisphere were shown to

have a specific deficit in tasks that require semantic retrieval (Fiez et al., 1992) or grammatical production (Silveri et al., 1994; Zettin et al., 1997). The right cerebellar hemisphere is reciprocally connected to the left cerebral hemisphere via the right SCP and the right MCP. Our findings provide an independent support in healthy adults for the involvement of the right cerebellum in speech and language.

No significant correlations between the CPs and articulation rate in neurotypical adults

Articulation rate was not associated with the microstructural properties in any of the CPs among our sample of neurotypical adults (Table S4). Of particular relevance is the non-significant association between articulation rate and diffusivities within the left ICP (Figure 5), in agreement with our previous findings in an independent, smaller sample of neurotypical adults (Jossinger et al., 2021). In that study, articulation rate was associated with FA along the left ICP only in a group of adults with persistent developmental stuttering and not in age-matched fluent speakers (see Fig. 6 in Jossinger et al., 2021). The ICP, transmitting sensory feedback signals from the periphery to the cerebellum, was repeatedly implicated in encoding motor errors during various motor tasks, including reaching movements (Shadmehr, 2017) and locomotion (Jossinger et al., 2020), which are crucial for the formation and updating of speech-related internal models (Tourville & Guenther, 2011). It was suggested that adults who stutter rely too heavily on sensory feedback while they speak due to a noisy or insufficient internal model (Hickok et al., 2011; Max et al., 2004). In neurotypical adults, on the other hand, a well-functioning internal model may be sufficient for producing fast and fluent speech, thus diminishing the speakers' dependency on sensory feedback in order to produce adequate articulatory output.

An alternative explanation for the lack of correlation between articulation rate and the microstructural properties of the ICP may rest in the type of task used to evaluate articulation rate. In clinical populations, diagnosed with various speech disorders, articulation rate is typically calculated over audio recordings of an unstructured interview. In neurotypical speakers, however, natural speaking may be insufficient to challenge the articulatory system in order to reveal its underlying neural mechanisms. To cope with this limitation, future studies could use the Diadochokinetic rate (DDK), a task designed to stress the articulatory system by measuring how quickly a person can produce a series of alternating sounds.[1]

[1] We are thankful to an anonymous NOL Reviewer for this idea.

The involvement of the frontal aslant tract in speech fluency

The FAT connects two cerebral areas important for speech production: the posterior inferior frontal gyrus (also known as "Broca's area") with the pre-supplementary motor area (pre-SMA) and SMA (Catani et al., 2013). Accumulative evidence from the last decade, mostly from clinical data, suggests that the FAT is a key pathway for speech fluency, as detailed below. The current study supplies further anatomical evidence for the involvement of the FAT in the fluent production of speech.

The FAT mediates speaking rate in neurotypical adults

Our results show a positive correlation between diffusivity of the bilateral FAT and speaking rate in neurotypical adults (Figure 6a and b; Figure S4). Specifically, we found that adults who speak faster have higher mean FA within their left and right FAT, and lower MD within their right FAT. The involvement of the FAT in speaking was previously demonstrated in patients. Electrical stimulation of the FAT during neural surgery was shown to elicit speech arrest (Fujii et al., 2015; Kinoshita et al., 2015; Vassal et al., 2014). In patients with primary-progressive aphasia and in patients with multiple sclerosis, the microstructural properties of the FAT were correlated with measures of speech rate and verbal fluency (Blecher et al., 2019; Catani et al., 2013; Li et al., 2017). To the best of our knowledge, this is the first study that shows a direct involvement of the bilateral FAT in speech production among healthy subjects.

No significant correlation between the FAT and articulation rate in neurotypical adults

Although speaking rate and articulation rate are highly correlated (Figure 2b), the bilateral FAT was associated with speaking rate, but not with articulation rate, and the difference between these correlation coefficients was significant. These findings are in line with previous results showing a significant association between the left FAT and articulation rate only in adults with persistent developmental stuttering, not in neurotypical adults (Kronfeld-Duenias et al., 2016). A recent study, investigating the same sample of neurotypical adults reported here, found that the bilateral FAT was also implicated in a morphological task that requires overt speech, beyond the contribution of verbal fluency scores (Yablonski et al., 2021). Taken together, these findings suggest that, in neurotypical adults, the FAT contributes to higher-level aspects of language production, rather than to articulatory motor control per-se.

Interpreting the results in terms of tissue properties

Both FA and MD are modulated by multiple biological factors, such as axonal density, directional coherence, axonal diameter and myelin content, which may influence FA and MD in opposite directions (Assaf & Pasternak, 2008; Beaulieu, 2002; Jones et al., 2013). For example, tight axonal packing or elevated myelination which lead to better neuronal communication, would manifest in elevated FA but reduced MD in the same voxel. On the other hand, wider axonal diameter, promoting efficient conduction (Liewald et al., 2014), would result in reduced FA and elevated MD (Barazany et al., 2009; Horowitz et al., 2015). Broadly speaking, however, FA and MD are not negatively correlated across different pathways, and may therefore reflect different components of the underlying tissue (De Santis et al., 2014; Uddin et al., 2019).

In our data, better phonemic fluency and faster speaking rate are associated with higher FA values in the right SCP and the bilateral FAT, respectively. Such positive correlations may be mediated by axonal packing or myelination: elevated axonal packing (or myelin content) would lead to both higher FA and better conductance, hence better performance. In addition to the positive correlations observed with FA metrics, negative correlations between MD and speaking rate were detected in the right MCP and the right FAT. Following the same line of reasoning developed earlier, one scenario that could lead to this pattern of results suggests that tightly packed axons, which are linked to better performance, also restrict the overall diffusivity in a voxel, thus causing a reduction in the local MD values in association with improved performance.

In sum, the directions of the associations we found are internally consistent, and are compatible with some explanations in terms of tissue properties, and not with others. These explanations may be further tested with advanced quantitative MRI measures that are sensitive to the different biological factors comprising the tissue (Assaf et al., 2008; Assaf & Basser, 2005; Berman et al., 2019; Filo et al., 2019; Mezer & Yeatman, 2014).

Limitations

The current study takes a tract-based approach, in which we test a small number of pre-defined hypotheses using individualized tractography methods in native space. This approach limits the number of hypotheses tested, as adding more tracts to the analysis would increase the chances of false positive results. Here, we focused on the bilateral CPs and FAT that were previously associated with different aspects of speech fluency in clinical populations (Jossinger

et al., 2021; Kronfeld-Duenias et al., 2016). However, we do not rule out the possibility that other white matter tracts may also contribute to various aspects of speech production. Specifically, the basal ganglia were previously shown to be implicated in speech fluency, in both clinical and neurotypical populations (Booth et al., 2007; Chang & Guenther, 2020; Zenon & Olivier, 2014). Future studies will be needed to test whether basal ganglia connections underpin speech fluency in neurotypical speakers.

A second limitation concerns the location of the correlations along the right SCP and right MCP, which were found in the vicinity of the decussation. At the point of decussation, voxels are occupied by both right and left tracts, making it difficult to attribute the findings to either the left or the right tract. Considering that voxels in the decussation of the CPs contain two fiber orientations (as shown by Jeurissen et al., 2013), such voxels likely contain primarily the two crossing CPs (e.g., left and right SCP), uncontaminated by other tracts. Nonetheless, crossing fibers are known to affect (typically reduce) FA values (Fig. 1c-d). The FA drop near the decussation is not sufficient, however, to generate a significant correlation, as the significant results with FA at the vicinity of decussation were specific to the right SCP and were not shown in other pathways that contain decussating fibers. The effect of crossing fibers on MD in our data is less dramatic: MD profiles (particularly in the MCP and ICP, see Fig. S4c-f) are generally flatter compared to FA profiles (Fig. 1c-d). Therefore, the fact that we find a significant correlation with MD in the right MCP suggests that this effect is not driven only by crossing fibers.

Lastly, the current study, as any other study that identifies correlations in a sample of adults, cannot be conclusive about the direction of causality that underlies the effects. Future developmental and longitudinal studies will help in determining whether the variability in the microstructure of the CPs and the FAT derives the variability in speech fluency seen in adulthood, or perhaps the differences in microstructure arise as a result of other cognitive and motor tasks involved in speech fluency.

Conclusions

In conclusion, our findings support the involvement of the cerebellum in aspects of speech production that go beyond articulatory control, such as lexical access, pragmatic or syntactic generation. Using complex modeling and probabilistic tracking enabled us to follow the trajectory of the cerebro-cerebellar pathways as they decussate, and to detect novel associations

with speech fluency in these pathways. By evaluating multiple measures of speech fluency, our study makes an important contribution to the understanding of the neural basis of speech production in neurotypical adults.

REFERENCES

Ackermann, H., Vogel, M., Petersen, D., & Poremba, M. (1992). Speech deficits in ischaemic cerebellar lesions. *Journal of Neurology*, *239*, 223–227.

Akers, D. (2006). CINCH. *Proceedings of the 19th Annual ACM Symposium on User Interface Software and Technology - UIST '06*, 33.

Ambrose, N. G., & Yairi, E. (1999). Normative disfluency data for early childhood stuttering. *Journal of Speech, Language, and Hearing Research : JSLHR*, *42*(4), 895–909.

Amir, O. (2016). Speaking Rate among Adult Hebrew Speakers: A Preliminary Observation. *Annals of Behavioural Science*, *2*(1), 1–9.

Amir, O., & Grinfeld, D. (2011). Articulation rate in childhood and adolescence: Hebrew speakers. *Language and Speech*, *54*(2), 225–240.

Amunts, J., Camilleri, J. A., Eickhoff, S. B., Heim, S., & Weis, S. (2020). Executive functions predict verbal fluency scores in healthy participants. *Scientific Reports*, *10*(1), 1–11.

Andrade, C. R. F., Maluf Cervone, L., & Chiarion Sassi, F. (2003). Relationship between the stuttering severity index and speech rate. *Sao Paulo Medical Journal*, *121*(2), 81–84.

Argyropoulos, G. P. D. (2016). The cerebellum, internal models and prediction in 'non-motor' aspects of language: A critical review. *Brain and Language*, *161*, 4–17.

Assaf, Y., & Basser, P. J. (2005). Composite hindered and restricted model of diffusion (CHARMED) MR imaging of the human brain. *NeuroImage*, *27*(1), 48–58.

Assaf, Y., Blumenfeld-Katzir, T., Yovel, Y., & Basser, P. J. (2008). AxCaliber: A method for measuring axon diameter distribution from diffusion MRI. *Magnetic Resonance in Medicine*, *59*(6), 1347–1354.

Assaf, Y., & Pasternak, O. (2008). Diffusion tensor imaging (DTI)-based white matter mapping in brain research: A review. *Journal of Molecular Neuroscience*, *34*(1), 51–61.

Barazany, D., Basser, P. J., & Assaf, Y. (2009). In vivo measurement of axon diameter

distribution in the corpus callosum of rat brain. *Brain*, *132*(5), 1210–1220.

Basser, P. J., & Pierpaoli, C. (1996). Microstructural and Physiological Features of Tissues Elucidated by Quantitative-Diffusion-Tensor MRI. *Journal of Magnetic Resonance, Series B*, *111*(3), 209–219.

Beaulieu, C. (2002). The basis of anisotropic water diffusion in the nervous system - a technical review. *NMR in Biomedicine*, *15*(7–8), 435–455.

Benjamini, Y., & Hochberg, Y. (1995). Controlling the false discovery rate: A practical and powerful approach to multiple testing. *Journal of the Royal Statistical Society Series B (Methodological)*, *57*(1), 289–300.

Berman, S., Filo, S., & Mezer, A. A. (2019). Modeling conduction delays in the corpus callosum using MRI-measured g-ratio. *NeuroImage*, *195*(November 2018), 128–139.

Blecher, T., Miron, S., Schneider, G. G., Achiron, A., & Ben-Shachar, M. (2019). Association between white matter microstructure and verbal fluency in patients with multiple sclerosis. *Frontiers in Psychology*, *10*(JULY).

Booth, J. R., Wood, L., Lu, D., Houk, J. C., & Bitan, T. (2007). The role of the basal ganglia and cerebellum in language processing. *Brain Research*, *1133*(1), 136–144.

Bose, A., Patra, A., Antoniou, G. E., Stickland, R. C., & Belke, E. (2022). Verbal fluency difficulties in aphasia: A combination of lexical and executive control deficits. *International Journal of Language & Communication Disorders*.

Bruckert, L., Shpanskaya, K., McKenna, E. S., Borchers, L. R., Yablonski, M., Blecher, T., Ben-Shachar, M., Travis, K. E., Feldman, H. M., & Yeom, K. W. (2019). Age-Dependent White Matter Characteristics of the Cerebellar Peduncles from Infancy Through Adolescence. *The Cerebellum*, *18*(3), 372–387.

Bruckert, L., Travis, K. E., Mezer, A. A., Ben-Shachar, M., & Feldman, H. M. (2020). Associations of Reading Efficiency with White Matter Properties of the Cerebellar Peduncles in Children. *Cerebellum*, *19*(6), 771–777.

Castellazzi, G., Bruno, S. D., Toosy, A. T., Casiraghi, L., Palesi, F., Savini, G., D'Angelo, E., & Wheeler-Kingshott, C. A. M. G. (2018). Prominent changes in cerebro-cerebellar functional connectivity during continuous cognitive processing. *Frontiers in Cellular Neuroscience*, *12*(October), 1–15.

Catani, M., Dell'Acqua, F., Vergani, F., Malik, F., Hodge, H., Roy, P., Valabregue, R., & Thiebaut de Schotten, M. (2012). Short frontal lobe connections of the human brain. *Cortex*, *48*(2), 273–291.

Catani, M., Mesulam, M. M., Jakobsen, E., Malik, F., Martersteck, A., Wieneke, C., Thompson, C. K., Thiebaut De Schotten, M., Dell'Acqua, F., Weintraub, S., & Rogalski, E. (2013). A novel frontal pathway underlies verbal fluency in primary progressive aphasia. *Brain*, *136*(8), 2619–2628.

Chang, L. C., Jones, D. K., & Pierpaoli, C. (2005). RESTORE: Robust estimation of tensors by outlier rejection. *Magnetic Resonance in Medicine*, *53*(5), 1088–1095.

Chang, S. E., & Guenther, F. H. (2020). Involvement of the Cortico-Basal Ganglia-Thalamocortical Loop in Developmental Stuttering. *Frontiers in Psychology*, *10*(January).

Connally, E. L., Ward, D., Howell, P., & Watkins, K. E. (2014). Disrupted white matter in language and motor tracts in developmental stuttering. *Brain and Language*, *131*, 25–35.

Costello, J. M., & Ingham, R. (1984). Assessment strategies for stuttering. In R. F. Curlee & W. H. Perkins (Eds.), *Nature and treatment of stuttering: New directions* (pp. 303–333). College Hill Press.

De Santis, S., Assaf, Y., Evans, C. J., & Jones, D. K. (2014). Improved precision in CHARMED assessment of white matter through sampling scheme optimization and model parsimony testing. *Magnetic Resonance in Medicine*, *71*(2), 661–671.

Fiez, J. A., Petersen, S., Cheney, M. K., & Raichle, M. E. (1992). Imparied non-motor learning and error detection associated with cerebellar damage. *Brain*, *115*(1), 155–178.

Filo, S., Shtangel, O., Salamon, N., Kol, A., Weisinger, B., Shifman, S., & Mezer, A. A. (2019). Disentangling molecular alterations from water-content changes in the aging human brain using quantitative MRI. *Nature Communications*, *10*(1), 3403.

Fonov, V., Evans, A. C., Botteron, K., Almli, C. R., McKinstry, R. C., & Collins, D. L. (2011). Unbiased average age-appropriate atlases for pediatric studies. *NeuroImage*, *54*(1), 313–327.

Friedman, L., Kenny, J. T., Wise, A. L., Wu, D., Stuve, T. A., Miller, D. A., Jesberger, J. A., & Lewin, J. S. (1998). Brain Activation During Silent Word Generation Evaluated with Functional MRI. *Brain and Language*, *64*(2), 231–256.

Fujii, M., Maesawa, S., Motomura, K., Futamura, M., Hayashi, Y., Koba, I., & Wakabayashi, T. (2015). Intraoperative subcortical mapping of a language-associated deep frontal tract connecting the superior frontal gyrus to Broca's area in the dominant hemisphere of patients with glioma. *Journal of Neurosurgery*, *122*(6), 1390–1396.

Guenther, F. H. (2006). Cortical interactions underlying the production of speech sounds. *Journal of Communication Disorders*, *39*(5), 350–365.

Gurd, J. M., Amunts, K., Weiss, P. H., Zafiris, O., Zilles, K., Marshall, J. C., & Fink, G. R. (2002). Posterior parietal cortex is implicated in continuous switching between verbal fluency tasks: an fMRI study with clinical implications. *Brain : A Journal of Neurology*, *125*(Pt 5), 1024–1038.

Halari, R., Sharma, T., Hines, M., Andrew, C., Simmons, A., & Kumari, V. (2006). Comparable fMRI activity with differential behavioural performance on mental rotation and overt verbal fluency tasks in healthy men and women. *Experimental Brain Research*, *169*(1), 1–14.

Henry, J. D., & Crawford, J. R. (2004). Verbal fluency deficits in Parkinson's disease: A meta-analysis. *Journal of the International Neuropsychological Society*, *10*(4), 608–622.

Hickok, G. (2012). Computatinal neuroanatomy of speech production. *Nature Reviews Neuroscience.*, *13*(2), 135-145.

Hickok, G., Houde, J., & Rong, F. (2011). Sensorimotor Integration in Speech Processing: Computational Basis and Neural Organization. *Neuron*, *69*(3), 407–422.

Horowitz, A., Barazany, D., Tavor, I., Bernstein, M., Yovel, G., & Assaf, Y. (2015). In vivo correlation between axon diameter and conduction velocity in the human brain. *Brain Structure and Function*, *220*(3), 1777–1788.

Howell, P., Au-Yeung, J., & Pilgrim, L. (1999). Utterance rate and linguistic properties as determinants of lexical dysfluencies in children who stutter. *Journal of the Acoustical Society of America*, *105*, 481–490.

Hubrich-Ungureanu, P., Kaemmerer, N., Henn, F. A., & Braus, D. F. (2002). Lateralized organization of the cerebellum in a silent verbal fluency task: A functional magnetic resonance imaging study in healthy volunteers. *Neuroscience Letters*, *319*(2), 91–94.

Ito, M. (2008). Control of mental activities by internal models in the cerebellum. *Nature Reviews Neuroscience*, *9*(4), 304–313.

Jeurissen, B., Leemans, A., Tournier, J. D., Jones, D. K., & Sijbers, J. (2013). Investigating the prevalence of complex fiber configurations in white matter tissue with diffusion magnetic resonance imaging. *Human Brain Mapping*, *34*(11), 2747–2766.

Jeurissen, B., Tournier, J.-D., Dhollander, T., Connelly, A., & Sijbers, J. (2014). Multi-tissue constrained spherical deconvolution for improved analysis of multi-shell diffusion MRI data. *NeuroImage*, *103*, 411–426.

Johnson, C. A., Liu, Y., Waller, N., & Chang, S. E. (2022). Tract profiles of the cerebellar peduncles in children who stutter. *Brain Structure and Function*, *0123456789*.

Jones, D. K., Knösche, T. R., & Turner, R. (2013). White matter integrity, fiber count, and other fallacies: The do's and don'ts of diffusion MRI. *NeuroImage*, *73*, 239–254.

Jossinger, S., Kronfeld-Duenias, V., Zislis, A., Amir, O., & Ben-Shachar, M. (2021). Speech rate association with cerebellar white-matter diffusivity in adults with persistent developmental stuttering. *Brain Structure and Function*, *226*(3), 801–816.

Jossinger, S., Mawase, F., Ben-Shachar, M., & Shmuelof, L. (2020). Locomotor Adaptation Is Associated with Microstructural Properties of the Inferior Cerebellar Peduncle. *The Cerebellum*, *19*(3), 370–382.

Jossinger, S., Sares, A., Zislis, A., Sury, D., Gracco, V., & Ben-Shachar, M. (2022). White matter correlates of sensorimotor synchronization in persistent developmental stuttering. *Journal of Communication Disorders*, *95*(November 2021), 106169.

Kavé, G. (2006). The development of naming and word fluency: evidence from Hebrew-speaking children between ages 8 and 17. *Developmental Neuropsychology*, *29*(3), 493–508.

Kavé, G., & Knafo-Noam, A. (2015). Lifespan development of phonemic and semantic fluency: Universal increase, differential decrease. *Journal of Clinical and Experimental Neuropsychology*, *37*(7), 751–763.

Kawato, M. (1999). Internal models for motor control and trajectory planning. *Current Opinion in Neurobiology*, *9*(6), 718–727.

Kelly, R. M., & Strick, P. L. (2003). Cerebellar loops with motor cortex and prefrontal cortex of a nonhuman primate. *The Journal of Neuroscience : The Official Journal of the Society for Neuroscience*, *23*(23), 8432–8444.

Kent, R. D., Kent, J. F., & Rosenbek, J. C. (1987). Maximum Performance Tests of Speech Production. *Journal of Speech and Hearing Disorders*, *52*(4), 367–387.

Kent, R. D., & Rosenbek, J. C. (1983). Acoustic Patterns of Apraxia of Speech. *Journal of Speech, Language, and Hearing Research*, *26*(2), 231–249.

Kinoshita, M., de Champfleur, N. M., Deverdun, J., Moritz-Gasser, S., Herbet, G., & Duffau, H. (2015). Role of fronto-striatal tract and frontal aslant tract in movement and speech: an axonal mapping study. *Brain Structure and Function*, *220*(6), 3399–3412.

Kramer, J. H., Mungas, D., Possin, K. L., Rankin, K. P., Boxer, A. L., Rosen, H. J., Bostrom, A., Sinha, L., Berhel, A., & Widmeyer, M. (2014). NIH EXAMINER: Conceptualization and Development of an Executive Function Battery. *Journal of the International Neuropsychological Society*, *20*(1), 11–19.

Kronfeld-Duenias, V., Amir, O., Ezrati-Vinacour, R., Civier, O., & Ben-Shachar, M. (2016). The frontal aslant tract underlies speech fluency in persistent developmental stuttering. *Brain Structure and Function*, *221*(1), 365–381.

Kruper, J., Yeatman, J. D., Richie-Halford, A., Bloom, D., Grotheer, M., Caffarra, S., Kiar, G., Karipidis, I. I., Roy, E., Chandio, B. Q., Garyfallidis, E., & Rokem, A. (2021). Evaluating the Reliability of Human Brain White Matter Tractometry. *Aperture Neuro*, *2021*(1), 1–26.

Leemans, A., & Jones, D. K. (2009). The B -matrix must be rotated when correcting for subject motion in DTI data. *Magnetic Resonance in Medicine*, *61*(6), 1336–1349.

Leiner, H. C. (2010). Solving the mystery of the human cerebellum. *Neuropsychology Review*, *20*(3), 229–235.

Leiner, H. C., Leiner, A. L., & Dow, R. S. (1986). Does the cerebellum contribute to mental skills? *Behavioral Neuroscience*, *100*(4), 443–454.

Li, M., Zhang, Y., Song, L., Huang, R., Ding, J., Fang, Y., Xu, Y., & Han, Z. (2017). Structural connectivity subserving verbal fluency revealed by lesion-behavior mapping in stroke patients. *Neuropsychologia*, *101*(January), 85–96.

Libon, D. J., McMillan, C., Gunawardena, D., Powers, C., Massimo, L., Khan, A., Morgan, B., Farag, C., Richmond, L., Weinstein, J., Moore, P., Coslett, H. B., Chatterjee, A., Aguirre, G., & Grossman, M. (2009). Neurocognitive contributions to verbal fluency deficits in frontotemporal lobar degeneration. *Neurology*, *73*(7), 535–542.

Liewald, D., Miller, R., Logothetis, N., Wagner, H. J., & Schüz, A. (2014). Distribution of axon diameters in cortical white matter: an electron-microscopic study on three human brains and a macaque. *Biological Cybernetics*, *108*(5), 541–557.

Marien, P., Engelborghs, S., Fabbro, F., & De Deyn, P. P. (2001). The lateralized linguistic cerebellum: A review and a new hypothesis. *Brain and Language*, *79*(3), 580–600.

Max, L., Guenther, F., & Gracco, V. (2004). Unstable or insufficiently activated internal models and feedback-biased motor control as sources of dysfluency: A theoretical model of stuttering. *Contemporary Issues in Communication Science and Disorders*, *31*, 105–122.

Mehl, M. R., Vazire, S., Ramírez-Esparza, N., Slatcher, R. B., & Pennebaker, J. W. (2007). Are women really more talkative than men? *Science*, *317*(5834), 82.

Mezer, A., & Yeatman, J. D. (2014). Quantifying the local tissue volume and composition in individual brains with MRI. *Pediatric Nephrology*, *29*(7), 1231–1238.

Middleton, F. a, & Strick, P. L. (1994). Anatomical evidence for cerebellar and basal ganglia involvement in higher cognitive function. *Science*, *266*(5184), 458–461.

Nichols, T. E., & Holmes, A. P. (2002). Nonparametric permutation tests for functional neuroimaging: A primer with examples. *Human Brain Mapping*, *15*(1), 1–25.

Oishi, K., Faria, A., Jiang, H., Li, X., Akhter, K., Zhang, J., Hsu, J. T., Miller, M. I., van Zijl, P. C. M., Albert, M., Lyketsos, C. G., Woods, R., Toga, A. W., Pike, G. B., Rosa-Neto, P., Evans, A., Mazziotta, J., & Mori, S. (2009). Atlas-based whole brain white matter analysis using large deformation diffeomorphic metric mapping: Application to normal elderly and Alzheimer's disease participants. *NeuroImage*, *46*(2), 486–499.

Oldfield, R. C. (1971). The assessment and analysis of handedness: The Edinburgh inventory. *Neuropsychologia*, *9*(1), 97–113.

Palesi, F., De Rinaldis, A., Castellazzi, G., Calamante, F., Muhlert, N., Chard, D., Tournier, J. D., Magenes, G., D'Angelo, E., & Wheeler-Kingshott, C. A. M. G. (2017). Contralateral cortico-ponto-cerebellar pathways reconstruction in humans in vivo: Implications for reciprocal cerebro-cerebellar structural connectivity in motor and non-motor areas. *Scientific Reports*, *7*(1), 1–13.

Palesi, F., Tournier, J. D., Calamante, F., Muhlert, N., Castellazzi, G., Chard, D., D'Angelo, E., & Wheeler-Kingshott, C. A. M. (2015). Contralateral cerebello-thalamo-cortical pathways

with prominent involvement of associative areas in humans in vivo. *Brain Structure and Function*, *220*(6), 3369–3384.

Perrini, P., Tiezzi, G., Castagna, M., & Vannozzi, R. (2013). Three-dimensional microsurgical anatomy of cerebellar peduncles. *Neurosurgical Review*, *36*(2), 215–225.

Peterburs, J., Bellebaum, C., Koch, B., Schwarz, M., & Daum, I. (2010). Working memory and verbal fluency deficits following cerebellar lesions: Relation to interindividual differences in patient variables. *Cerebellum*, *9*(3), 375–383.

Petersen, S. E., Fox, P. T., Posner, M. I., Mintun, M., & Raichle, M. E. (1988). Positron emission tomographic studies of the cortical anatomy of single-word processing. *Nature*, *331*(6157), 585–589.

Petersen, S. E., Fox, P. T., Posner, M. I., Mintun, M., & Raichle, M. E. (1989). Positron Emission Tomographic Studies of the Processing of Singe Words. *Journal of Cognitive Neuroscience*, *1*(2), 153–170.

R Core Team. (2013). R: A language and environment for statistical computing. *R Foundation for Statistical Computing, Vienna, Austria.*

Riecker, A., Kassubek, J., Gröschel, K., Grodd, W., & Ackermann, H. (2006). The cerebral control of speech tempo: Opposite relationship between speaking rate and BOLD signal changes at striatal and cerebellar structures. *NeuroImage*, *29*(1), 46–53.

Riecker, A., Mathiak, K., Wildgruber, D., Erb, M., Hertrich, I., Grodd, W., & Ackermann, H. (2005). fMRI reveals two distinct cerebral networks subserving speech motor control. *Neurology*, *64*(4), 700–706.

Rochman, D., & Amir, O. (2013). Examining in-session expressions of emotions with speech/vocal acoustic measures: An introductory guide. *Psychotherapy Research*, *23*(4), 381–393.

Rodero, E. (2012). A comparative analysis of speech rate and perception in radio bulletins. *Text and Talk*, *32*(3), 391–411.

Rohde, G. K., Barnett, A. S., Basser, P. J., Marenco, S., & Pierpaoli, C. (2004). Comprehensive approach for correction of motion and distortion in diffusion-weighted MRI. *Magnetic Resonance in Medicine*, *51*(1), 103–114.

Schlösser, R., Hutchinson, M., Joseffer, S., Rusinek, H., Saarimaki, A., Stevenson, J., Dewey, S.

L., & Brodie, J. D. (1998). Functional magnetic resonance imaging of human brain activity in a verbal fluency task. *Journal of Neurology, Neurosurgery & Psychiatry* , *64*(4), 492–498.

Schmahmann, J. D. (2010). The role of the cerebellum in cognition and emotion: Personal reflections since 1982 on the dysmetria of thought hypothesis, and its historical evolution from theory to therapy. *Neuropsychology Review*, *20*(3), 236–260.

Shadmehr, R. (2017). Learning to Predict and Control the Physics of Our Movements. *The Journal of Neuroscience*, *37*(7), 1663–1671.

Shadmehr, R., & Krakauer, J. W. (2008). A computational neuroanatomy for motor control. *Experimental Brain Research*, *185*(3), 359–381.

Shao, Z., Janse, E., Visser, K., & Meyer, A. S. (2014). What do verbal fluency tasks measure? Predictors of verbal fluency performance in older adults. *Frontiers in Psychology*, *5*(JUL), 1–10.

Silveri, M. C., Leggio, M. G., & Molinari, M. (1994). The cerebellum contributes to linguistic production. *Neurology*, *44*(11), 2047–2047.

Sobczak-Edmans, M., Lo, Y. C., Hsu, Y. C., Chen, Y. J., Kwok, F. Y., Chuang, K. H., Tseng, W. Y. I., & Chen, S. H. A. (2019). Cerebro-Cerebellar Pathways for Verbal Working Memory. *Frontiers in Human Neuroscience*, *12*(January), 1–13.

Sturm, J., & Seery, C. H. (2007). Speech and articulatory rates of school-age children in conversation and narrative contexts. *Language, Speech, and Hearing Services in Schools*, *38*(1), 47–59.

Tournier, J. D., Calamante, F., & Connelly, A. (2007). Robust determination of the fibre orientation distribution in diffusion MRI: Non-negativity constrained super-resolved spherical deconvolution. *NeuroImage*, *35*(4), 1459–1472.

Tournier, J. D., Calamante, F., Gadian, D. G., & Connelly, A. (2004). Direct estimation of the fiber orientation density function from diffusion-weighted MRI data using spherical deconvolution. *NeuroImage*, *23*(3), 1176–1185.

Tournier, J. D., Smith, R., Raffelt, D., Tabbara, R., Dhollander, T., Pietsch, M., Christiaens, D., Jeurissen, B., Yeh, C.-H., & Connelly, A. (2019). MRtrix3: A fast, flexible and open software framework for medical image processing and visualisation. *NeuroImage*, *202*,

116137.

Tourville, J. A., & Guenther, F. H. (2011). The DIVA model: A neural theory of speech acquisition and production. *Language and Cognitive Processes*, *26*(7), 952–981.

Travis, K. E., Leitner, Y., Feldman, H. M., & Ben-Shachar, M. (2015). Cerebellar white matter pathways are associated with reading skills in children and adolescents. *Human Brain Mapping*, *36*(4), 1536–1553.

Tuch, D. S., Reese, T. G., Wiegell, M. R., & Wedeen, V. J. (2003). Diffusion MRI of Complex Neural Architecture. *Neuron*, *40*(5), 885–895.

Uddin, M. N., Figley, T. D., Solar, K. G., Shatil, A. S., & Figley, C. R. (2019). Comparisons between multi-component myelin water fraction, T1w/T2w ratio, and diffusion tensor imaging measures in healthy human brain structures. *Scientific Reports*, *9*(1), 2500.

Vassal, F., Boutet, C., Lemaire, J.-J., & Nuti, C. (2014). New insights into the functional significance of the frontal aslant tract: An anatomo–functional study using intraoperative electrical stimulations combined with diffusion tensor imaging-based fiber tracking. *British Journal of Neurosurgery*, *28*(5), 685–687.

Walker, J. F., Archibald, L. M. D., Cherniak, S. R., & Fish, V. G. (1992). Articulation Rate in 3- and 5-Year-Old Children. *Journal of Speech, Language, and Hearing Research*, *35*(1), 4–13.

Wells, W., Viola, P., Atsumi, H., Nakajima, S., & Kikinis, R. (1996). Multi-modal volume registration by maximization of mutual information. *Medical Image Analysis*, *1*(1), 35–51.

Wolpert, D. M., Miall, R. C., & Kawato, M. (1998). Internal models in the cerebellum. *Trends in Cognitive Sciences*, *2*(9), 338–347.

Xie, J., Cai, T. T., Maris, J., & Li, H. (2011). Optimal false discovery rate control for dependent data. *Statistics and Its Interface*, *4*(4), 417–430.

Yablonski, M., & Ben-Shachar, M. (2020). Sensitivity to word structure in adult Hebrew readers is associated with microstructure of the ventral reading pathways. *Cortex*, *128*, 234–253.

Yablonski, M., Menashe, B., & Ben-Shachar, M. (2021). A general role for ventral white matter pathways in morphological processing: Going beyond reading. *NeuroImage*, *226*(June 2020), 117577.

Yeatman, J. D., Dougherty, R. F., Myall, N. J., Wandell, B. A., & Feldman, H. M. (2012). Tract

Profiles of White Matter Properties: Automating Fiber-Tract Quantification. *PLoS ONE*, *7*(11), e49790.

Yeatman, J. D., Dougherty, R. F., Rykhlevskaia, E., Sherbondy, A. J., Deutsch, G. K., Wandell, B. A., & Ben-Shachar, M. (2011). Anatomical Properties of the Arcuate Fasciculus Predict Phonological and Reading Skills in Children. *Journal of Cognitive Neuroscience*, *23*(11), 3304–3317.

Zenon, A., & Olivier, E. (2014). Contribution of the basal ganglia to spoken language: Is speech production like the other motor skills? *Behavioral and Brain Sciences*, *37*(6), 576–576.

Zettin, M., Cappa, S. F., D'amico, A., Rago, R., Perino, C., Perani, D., & Fazio, F. (1997). Agrammatic speech production after a right cerebellar haemorrhage. *Neurocase*, *3*(5), 375–380.